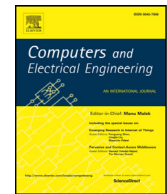




Contents lists available at ScienceDirect

## Computers and Electrical Engineering

journal homepage: [www.elsevier.com/locate/compeleceng](http://www.elsevier.com/locate/compeleceng)Slit-type one-dimensional brightness distribution sensor for object tracking<sup>☆</sup>Shota Nakashima<sup>a,\*</sup>, Shenglin Mu<sup>b</sup>, Shingo Aramaki<sup>a</sup>, Yuhki Kitazono<sup>c</sup>,  
Kanya Tanaka<sup>a</sup><sup>a</sup> Graduate School of Sciences and Technology for Innovation, Yamaguchi University, 2-16-1, Tokiwadai, Ube-city, Yamaguchi, 755-8611, Japan<sup>b</sup> Department of Electronic Control Engineering, National Institution of Technology, Hiroshima College, 4272-1, Higashino, Osakikamijima-cho, Toyota-gun, Hiroshima, 725-0231, Japan<sup>c</sup> Department of Creative Engineering, National Institute of Technology, Kitakyushu College, 5-20-1, Shii, Kokuraminami-ku, Kitakyushu-city, Fukuoka, 802-0985, Japan

## ARTICLE INFO

## Article history:

Received 26 May 2016

Revised 17 September 2016

Accepted 19 September 2016

Available online xxx

## Keywords:

Obrid-Sensor

Brightness distribution

Computational imaging

Safety confirmation

Object tracking

## ABSTRACT

This paper presents a novel computational imaging method for object tracking. The proposed slit-type one-dimensional brightness distribution sensor (Obrid-Sensor) is designed to be applied to detect falls, localize, and track subjects without invading privacy. According to the vertical and horizontal one-dimensional brightness distributions acquired by the proposed sensors, the subject's motion is monitored without images or videos. The effectiveness of the proposed method to detect falls, localize, and track is verified by experiment. The motion detection and location can be implemented without requiring images or videos, which may invade privacy. The detection range of the proposed privacy-preserving sensor is also confirmed. Finally, the proposed sensor has a simpler structure than the traditional Obrid-Sensor, making it attractive owing to its simple design, facile application, and low cost.

© 2016 The Authors. Published by Elsevier Ltd.

This is an open access article under the CC BY-NC-ND license

(<http://creativecommons.org/licenses/by-nc-nd/4.0/>).

## 1. Introduction

In recent years, the average age of the population has been growing rapidly not only in developed countries, but also throughout the entire world, leading to many serious problems, particularly in the medical and welfare fields, where numerous problems need attention. In Japan, the developed country with the most acute aging problem, an urgent need exists for more people to care for the elder population. Because of the increasing number of elders, such work is becoming harder and harder. For example, a significant labor force is required just to confirm the safety of elders in their daily life. To further complicate matters, accidents involving elders, such as falls, can lead to serious consequences such as bad injuries or even death. Safety-confirmation systems are thus necessary and important for relieving the burden of care workers. To address this need, recent research has developed systems with cameras. For example, Benezeth et al., Paul et al., and Vineet et al.

<sup>☆</sup> This paper is for CAEE special section SI-aicv. Reviews processed and recommended for publication to the Editor-in-Chief by Guest Editor Dr. H. Lu.

\* Corresponding author.

E-mail addresses: [s-naka@yamaguchi-u.ac.jp](mailto:s-naka@yamaguchi-u.ac.jp) (S. Nakashima), [mshenglin@hiroshima-cmt.ac.jp](mailto:mshenglin@hiroshima-cmt.ac.jp) (S. Mu), [w001wc@yamaguchi-u.ac.jp](mailto:w001wc@yamaguchi-u.ac.jp) (S. Aramaki), [kitazono@kct.ac.jp](mailto:kitazono@kct.ac.jp) (Y. Kitazono), [ktanaka@yamaguchi-u.ac.jp](mailto:ktanaka@yamaguchi-u.ac.jp) (K. Tanaka).<http://dx.doi.org/10.1016/j.compeleceng.2016.09.023>

0045-7906/© 2016 The Authors. Published by Elsevier Ltd. This is an open access article under the CC BY-NC-ND license

(<http://creativecommons.org/licenses/by-nc-nd/4.0/>).

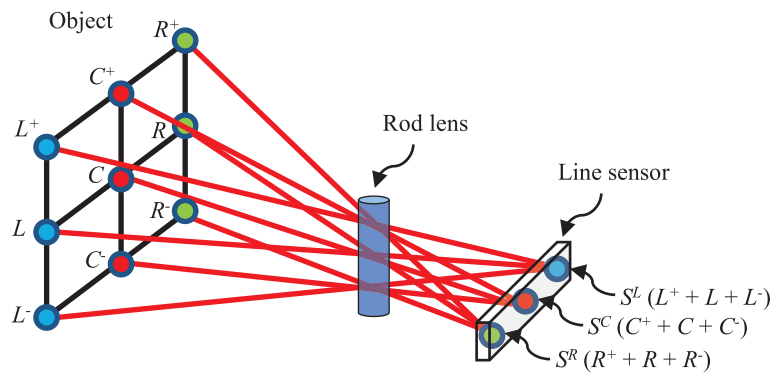


Fig. 1. Rod-lens-type Obrid Sensor.

[1–3] proposed methods for detecting human presence by using surveillance cameras. The method of Benezh et al. detects human presence in an indoor environment by combining a background-subtraction algorithm, tracking, and recognition. The method of Paul et al. detects moving objects by using shape-based, texture-based, or motion-based features. The method of Vineet et al. detects human presence by using instance-based human segmentation. However, such conventional systems based on surveillance cameras have several limitations, such as high cost and being difficult to use. In particular, because of privacy protection policies, normal surveillance systems with cameras are not applicable in private living quarters, where falling accidents often happen. In addition, although some camera-based methods have integrated privacy-preservation algorithms, such systems are difficult for users to accept [4–6]. Therefore, a dire need exists for a camera-free system that can detect position and movement status and track subjects to confirm their safety.

Various sensing technologies have been proposed for motion detection [7–9]. For example, Osada et al. proposed a sensing system involving multiple pyroelectric sensors [10]. The system is designed to be fixed in an array to the ceiling to detect subject motion, which requires that the room be refitted—bringing with it the concomitant costs. Another system uses tags that emit electromagnetic waves. In this method, the subject attached tags to his or her body to allow their motion to be detected and tracked, within a given range, by a tag reader. Unfortunately, attaching these tags is not an easy task to incorporate into daily life. In addition, some subjects do not appreciate the encumbrance involved in wearing electronic devices all day. Moreover, the electromagnetic waves may cause unexpected effects on subjects with pacemakers. Yet another detection method is based on smart phones. Based on information acquired via sensors within a subject's smart phone, the subject status can be detected. However, this method is also limited in that it requires smart phones with the proper sensors, and the subject's motion can only be monitored when the smart phone is present.

To solve the problems, we developed a sensor in previous research that can localize a subject without invading privacy [11,12]. The proposed method localizes the subject by integrating along a vertical line of pixels in a two-dimensional image instead of by using a one-dimensional brightness distribution obtained by combining a line sensor and a cylindrical lens. Experiment show that this proposed method detects the subject's presence, position, and movement status, the all without invading privacy. In addition, this method can track the subjects without invading their privacy.

This present paper presents a computational imaging method for object tracking. The proposed slit-type one-dimensional brightness distribution sensor (Obrid-Sensor) is designed to be used to detect falls, localize, and track subjects without invading privacy. This research involved fabricating the sensor and testing it in the field. The effectiveness of the proposed method for fall detection, localization, and object tracking is verified by experiment. Motion detection and location is accomplished without requiring images or videos, which cause privacy problems. In addition, the detection range of the proposed privacy-preserving sensor is confirmed.

The paper is organized as follows: Section 2 explains the theoretical structure of a one-dimensional brightness distribution sensor and the model for acquiring the brightness distribution. Next, the experiments are discussed in Section 3. Finally, the conclusions are given in the last section.

## 2. Theoretical structure of Obrid-sensor

As opposed to the rod-lens-type Obrid-Sensor proposed in previous research [13], we propose herein a slit-type Obrid-Sensor that can acquire a one-dimensional brightness distribution by combining the signal from a line sensor positioned parallel to a slit through which light passes. The proposed privacy-preserving sensor can detect the subject's status without requiring cameras or other video equipment. Based on the results of simulations that use the brightness distribution from a two-dimensional image captured by a camera, we verify the effectiveness of the proposed design. Thus, in this work, we implemented the sensor system and confirmed its effectiveness experimentally via field tests.

Figs. 1 and 2 show the theoretical structure of a traditional Obrid-Sensor, which is constructed with a line sensor and a rod lens. The rod lens has the same properties as the cylindrical lens that finds use in facsimiles, scanners, printers, etc. [11]. Figs. 3 and 4 show the theoretical structure of a slit-type Obrid-Sensor. Instead, of using a rod lens as condenser, the slit-type Obrid-Sensor uses a slit to create a one-dimensional image.

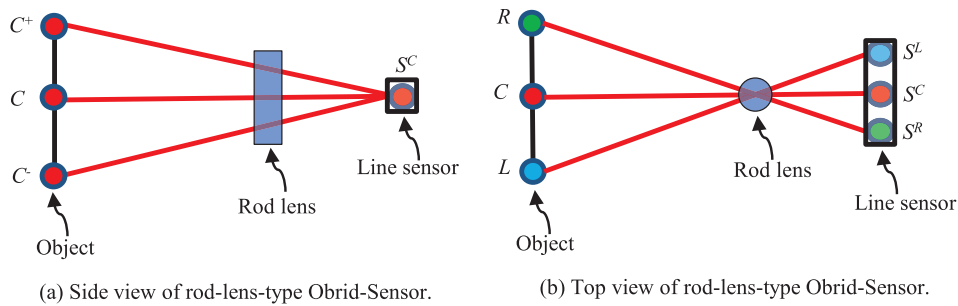


Fig. 2. Different views of rod-lens-type Obrid Sensor.

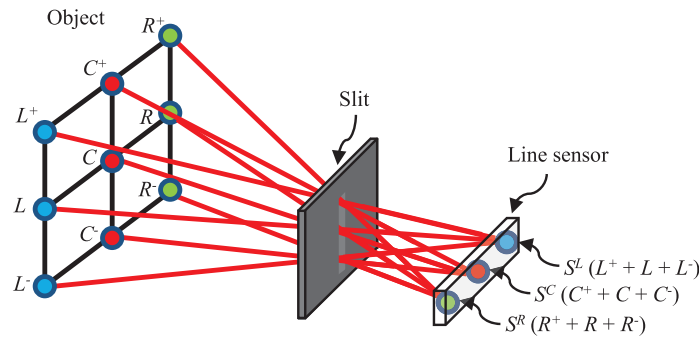


Fig. 3. Slit-type Obrid Sensor.

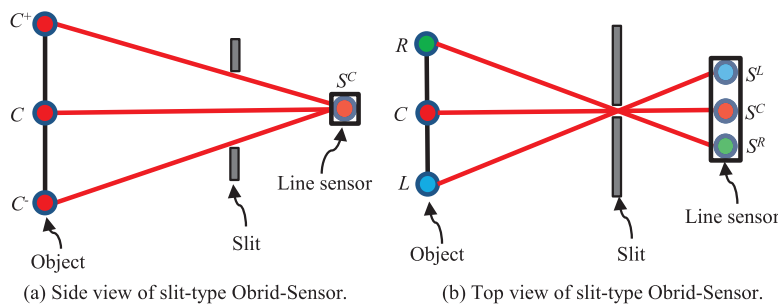


Fig. 4. Different views of slit-type Obrid Sensor.

The slit-type Obrid-Sensor is designed to detect a subject's status without using video or image information. The grid appearing in the left part of Figs. 1 and 3 is used to express an object. In horizontal direction, the object is divided into a left part (blue), a center part (red), and a right part (green), as denoted by  $L$ ,  $C$ , and  $R$ . In vertical direction, the height of the object is marked from high to low by a plus sign, no sign, and a minus sign. This way, the object can be expressed in two dimensions. Light from each part of the object goes through the side surface of the rod lens, which is positioned with respect to the line sensor as shown in the figure. On the one hand, the light from the left part of the object arrives at the right part of the line sensor, as expressed by  $S^R$ . Light from the right part of the object arrives at the left part of the line sensor, as expressed by  $S^L$ . Finally, light from the middle of the object arrives at the center part of the line sensor, as expressed by  $S^C$ . On the other hand, light along a vertical line is concentrated onto the one-dimensional line sensor. Fig. 2(a) shows a cut-away side view at the center of the object. Fig. 2(b) shows the top view. According to the structure as shown in Fig. 1, the Obrid-Sensor can detect a subject's horizontal position and horizontal movement. Thus, the sensor was applied to localizing and tracking a subject indoors. In addition, when we use the sensor for actual detection, it can be rotated by  $90^\circ$  about the line  $C$ - $S^C$ . In this way, the Obrid-Sensor can be applied to detect variations in brightness distribution in the vertical direction. By exploiting such variations, we can detect the motion of subject in the vertical direction (i.e., standing, sitting, or falling) [13].

In this paper, we propose a slit-type Obrid-Sensor based on our previous research. This sensor uses a slit-type cover instead of a conventional rod lens. In comparison with the traditional rod-lens-type Obrid-Sensor, the proposed sensor is costs less and is more flexible for practical applications. Fig. 3 shows the structure of the slit in the figure; the proposed structure involves a dark-blue mask to define the slit. Theoretically, the slit should be opaque so as to block all light except

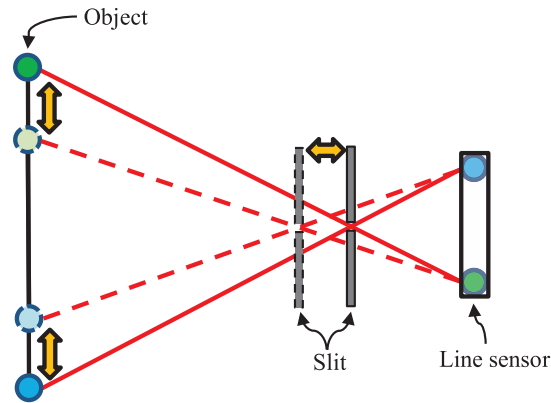


Fig. 5. Flexibility in design of slit-type Obrid Sensor.

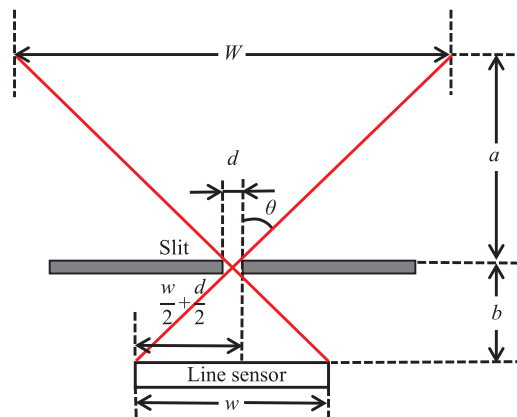


Fig. 6. Geometry used to estimate detection range for slit-type Obrid Sensor.

that coming through the slit. Fig. 4(a) shows a cut-away side view at center position of the slit-type Obrid-Sensor. Light in the vertical direction is concentrated onto the line sensor without requiring a rod lens. Fig. 4(b) shows the top view of the slit-type Obrid-Sensor. Lights in the horizontal direction goes through the slit in the same way as it goes through a conventional rod-lens-type sensor. Applying the slit-type structure leads to a more flexible design of the Obrid-Sensor.

Fig. 5 shows the flexibility for setting the horizontal detection range by adjusting the distance between the slit and the line sensor. The figure shows two light rays (solid and dashed line, respectively). The solid lines show the light rays when the slit is at the correct position; that is, when the slit is closer to the line sensor. For a constant distance between the object and the line sensor, a wider object (i.e., from the green point to the blue point in horizontal direction) can be detected, as shown in Fig. 5. In other words, the detection range is larger in the horizontal direction when the focus is shorter. In contrast with the rod-lens-type Obrid-Sensor, the proposed design is not limited by the focal length of the lens. In real applications, the sensor can be adjusted according to specific requirements.

Fig. 6 shows the basic design theory of the slit-type Obrid-Sensor. Its detection angle can be determined by using Eq. 1, where  $d$  is the slit width,  $a$  is the distance between object and slit,  $b$  is the distance between slit and line sensor, and  $w$  is the width of the line sensor. The theory indicates that the slit-type Obrid-Sensor is more flexible than the rod-lens-type Obrid-Sensor.

$$\theta = \tan^{-1} \left( \frac{2b}{w + d} \right) \quad (1)$$

$$w = 2a \cdot \tan \theta \quad (2)$$

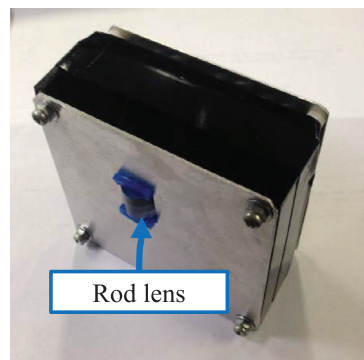
### 3. Experiments and discussion

#### 3.1. Evaluation of proposed sensor

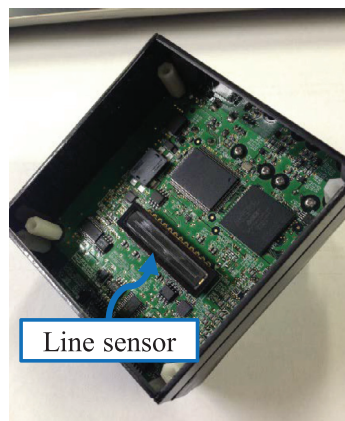
To verify the usefulness of the proposed sensor, we conducted experiments in which, as shown in Fig. 6, the detection range could be set according to the given requirements. In this research, the Obrid-Sensor was implemented by using a



(a) Appearance of slit-type Obrid-Sensor.



(b) Appearance of rod-lens-type Obrid-Sensor.



(c) Line sensor in Obrid-Sensor.

**Fig. 7.** Structures of slit- and rod-lens-type Obrid Sensor.

14.336 mm  $\times$  0.224 mm Hamamatsu Photonics K.K. CCDS11071-1104 line sensor [see Fig. 7(c)]. The line sensor is connected to a Hamamatsu Photonics K.K. C11288 drive circuit, which converts analog video signals from a CCD into digital signals and outputs them. The USB connector (USB 2.0) provided as a standard feature facilitates connection to a PC for controlling the drive circuit and data acquisition. Fig. 7(a) shows the structure of the slit-type Obrid-Sensor and Fig. 7(b) shows the structure of the rod-lens-type Obrid-Sensor. We used both in the experiments, and the distance  $b$  between line sensor and slit was set to 15.47 or 39.07 mm, respectively. Fig. 8 shows the experimental environment. Assuming the sensor is used in a normal living room for detection, the detecting distance  $a$  between the subject and the Obrid-Sensor can be set to 2.00 m as a benchmark distance. The detection range  $W$  in the horizontal direction can be measured when the subject moves from point a to c. Fig. 9(a) and (b) show photographs of experiments in two different detection range. Table 1 presents the experimental results for the detection range as a function of the different distances  $b$  between the slit and the line sensor. According to

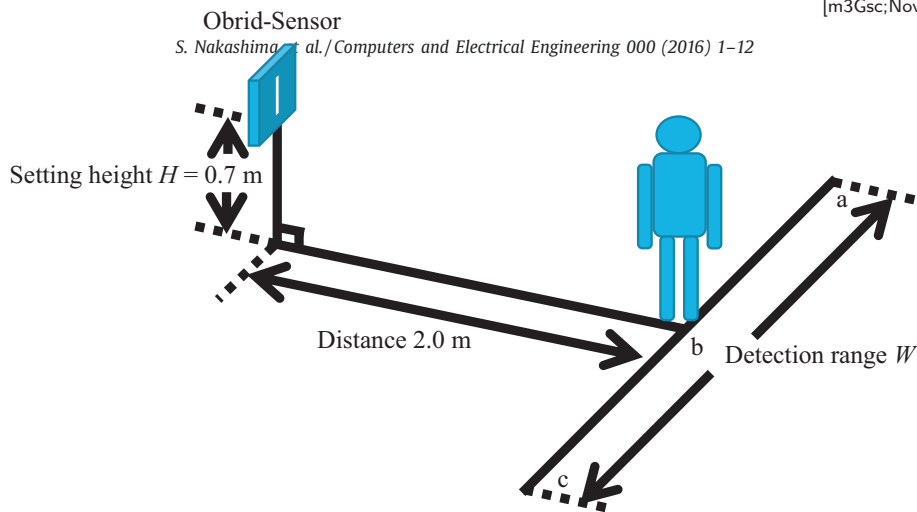
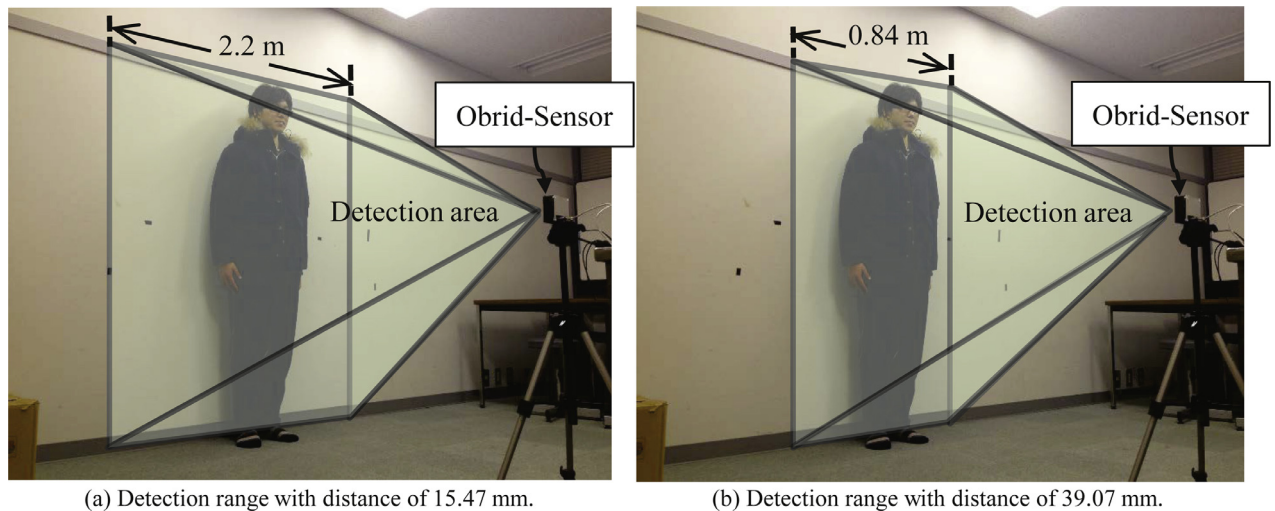


Fig. 8. Experimental environment.



(a) Detection range with distance of 15.47 mm.

(b) Detection range with distance of 39.07 mm.

Fig. 9. Detection ranges with different slit-sensor distances.

**Table 1**  
Experimental results.

Distance between slit and line sensor	Detection range $W$ [m]	
	Theoretical value	Experimental value
15.47 mm	1.90	2.20
39.07 mm	0.76	0.84

our estimates, when the slit-detector distance is 15.47 mm, the detection range should be 1.90 m. Experimentally, an object at 2.2 m range can be detected, which gives an error rate of 15.79%. For a slit-detector distance of 39.07 mm, the detection range should be 0.76 m, whereas the experimental range was 0.84 m, which gives an error rate of 10.53%.

The experimental ranges were greater than the theoretical ranges in both cases, which means that the design introduces factors that lengthen the detection range. Considering that the sensor used in the experiments was handmade, we feel that an error rate below 16% is acceptable. Based on these results, additional ranges were also determined experimentally, which shows clearly that the sensor can be used based on the theoretical detection range. In the experiments, a shorter (longer) object distance test led to a larger (smaller) error. In addition, if the distance  $b$  is long, the detection range is limited. Thus, the error decreases with increasing detection limit, the error decreases. Therefore, the object distance must be related to the error. More sample sensors will be made to verify this relationship.

Figs. 10–12 show the relationship of exact subject motions and the corresponding variations in brightness distribution. Panels (a) in the figures show the actual camera images in experiments. Panels (b) in the figures show the brightness



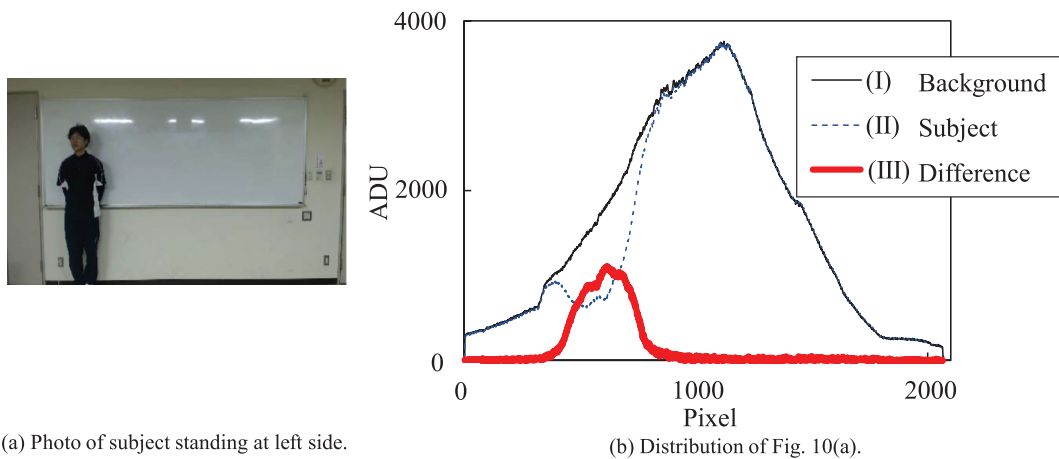


**Fig. 10.** Experimental situation with subject at left side and its distribution.

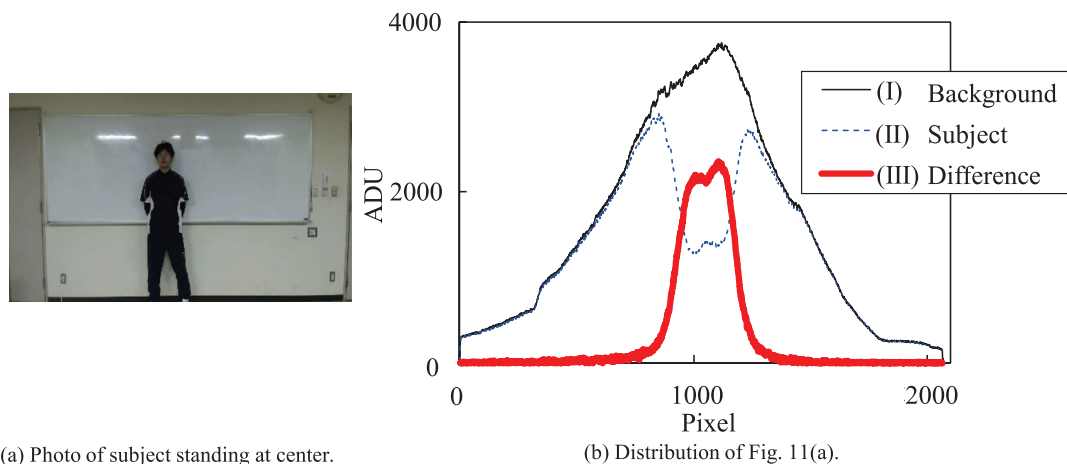


**Fig. 11.** Experimental situation with subject at center and corresponding distribution.

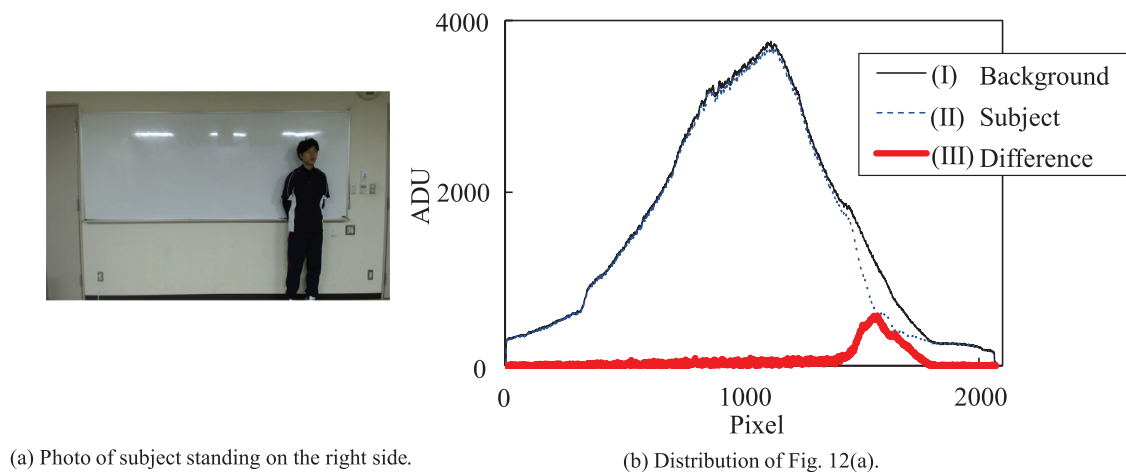


**Fig. 12.** Experimental situation with subject on the right side and corresponding distribution.

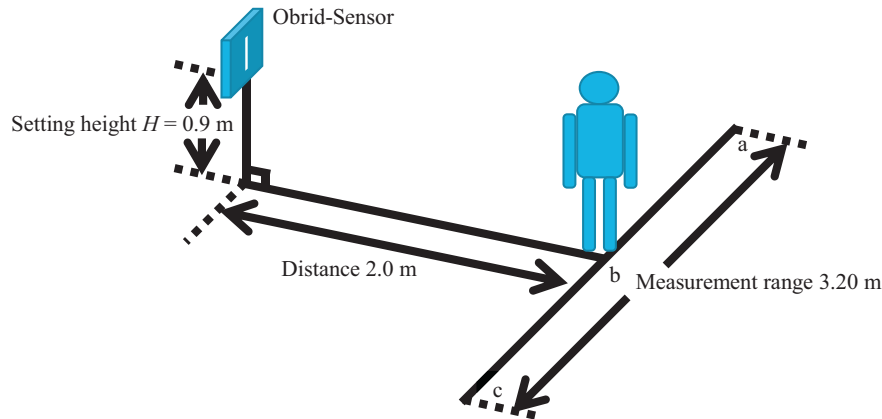


Fig. 13. Experimental environment.

**Table 2**  
Experimental conditions.

Sensor	Horizontal movement detection angle $\theta_{MD}$	87.06 deg
	Vertical integration detection angle $\theta_I$	26.99 deg
	Setting depression angle $\theta_D$	0 deg
	Setting height $H$	90 cm
Subject	Height $h$ (body height)	173 cm
	Width $w$	50 cm
	Color	White
Color of background		White
Illuminance of experimental environment		350 lx

distribution of the background acquired in the first step (line I) [13]. The dashed line (II) shows the brightness distribution with subject. The difference between brightness distributions of (I) and (II) is shown by line (III). The subject's feature quantity is included in line (III). Thus, the peak position of the subject's feature quantity in line (III) is interpreted as the subject's position. Figs. 10–12 show the results when the subject stands to the left, center, and right, respectively, in the detection range. It is clear that the brightness distribution moves horizontally following precisely the subject's motion. The subject's motion can thus be localized based on the difference in the brightness distribution acquired by the proposed slit-type Obrid-Sensor.

### 3.2. Verification experiment with small difference in brightness

The proposed Obrid-Sensor does not illuminate the subject, so the proposed sensor must detect the subject by using ambient light reflected from the subject. Thus, if the subject brightness is close to the background brightness, the sensor will have difficulty detecting the subject by using background subtraction. We thus designed an experiment to test the sensor under these difficult conditions. Fig. 13 shows the experimental environment and Table 2 gives the experimental conditions. The experiment involved acquiring the brightness distribution as the subject moved from left to right within the detection range. Figs. 14–16 show the experimental results. Because the subject's feature quantity is greater than the noise (other parts of subject's feature quantity), the sensor can detect the subject. We thus set the threshold to differentiate between the subject's feature quantity and the noise, which allows us to extract the subject's feature quantity according to this threshold. The peak position of the extracted feature quantity is interpreted as the subject's position. In Fig. 16, the threshold  $t_p = 3$  to differentiate between the subject's feature quantity and the noise. In addition, the peak position  $p = 1301$  for the subject's feature quantity, which gives the subject's position.

### 3.3. Experiment to detect standing and falling

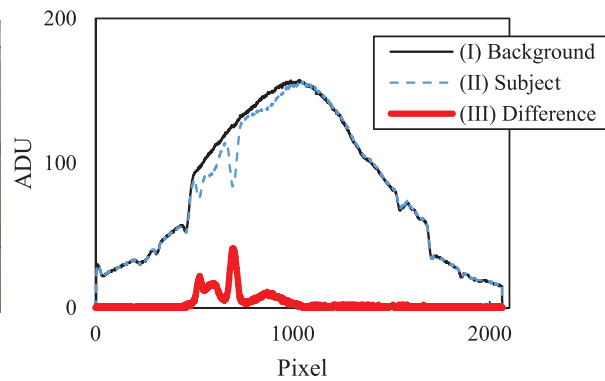
We conducted an experiment to detect standing and falling. In this experiment, the structure of Fig. 1 is rotated by  $90^\circ$  about the line C-S<sup>C</sup>. Thus, the Obrid-Sensor can detect motion in the vertical direction. Fig. 17 shows the experimental environment and Table 3 gives the experimental conditions. The experiment involved acquiring the brightness distribution as the subject stood or fell. Moreover, the center of gravity was derived from the brightness distribution.

Figs. 18 and 19 show the experimental results. When the subject was standing, the center of gravity  $g_s = 1064$ . However, when subject was falling, the center of gravity  $g_f = 693$ . Thus, if subject is standing (falling), the center of gravity position





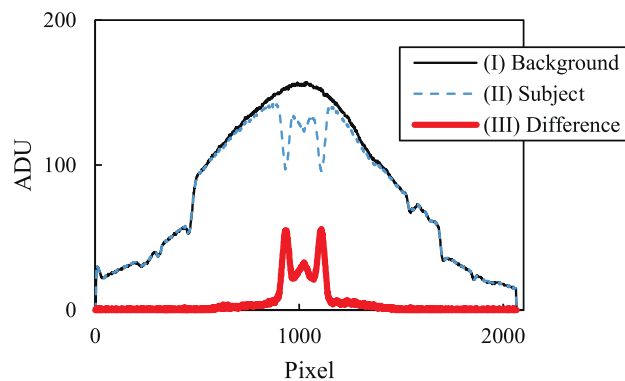
(a) Photo of subject standing on the left side.



(b) Distribution of Fig. 14(a).

**Fig. 14.** Experimental situation with subject on the left side and corresponding brightness distribution.

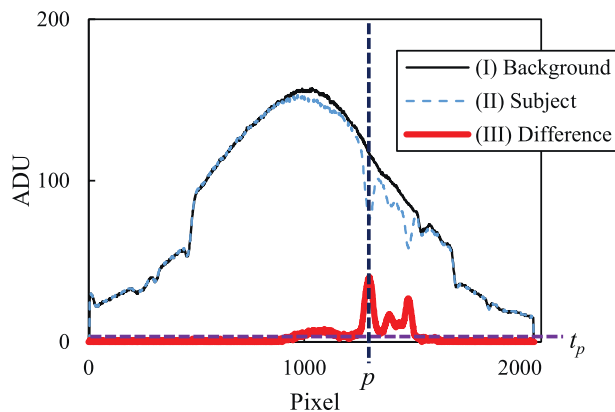
(a) Photo of subject standing in the center.



(b) Distribution of Fig. 15(a).

**Fig. 15.** Experimental situation with subject in the center and corresponding brightness distribution.

(a) Photo of subject standing on the right side.



(b) Distribution of Fig. 16(a).

**Fig. 16.** Experimental situation with subject on the right side and corresponding brightness distribution.

$g_s$  ( $g_f$ ) is high (low). Therefore, the sensor can detect whether the subject is standing or falling based on the change in the center of gravity of the feature.

#### 4. Conclusions

Significant research has been made in recent years to address the problem of an aging population. In this research, we propose a slit-type Obrid-Sensor that provides improved object tracking and safety for elders without perturbing their daily

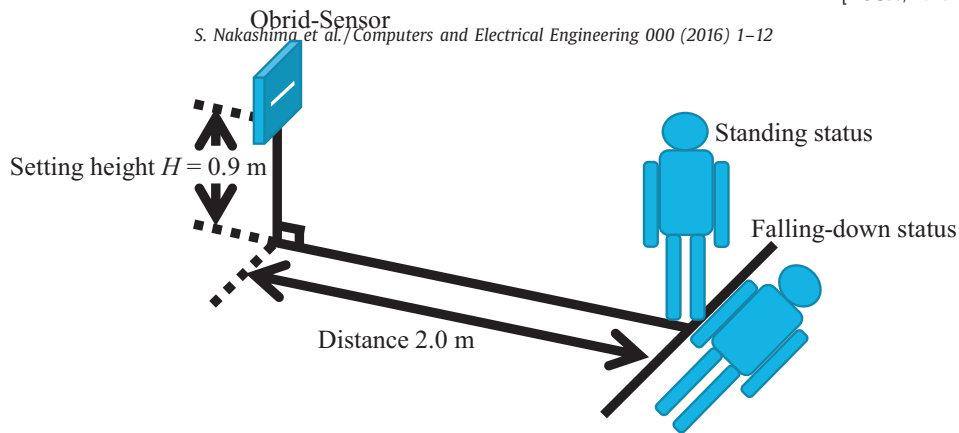


Fig. 17. Experimental environment.

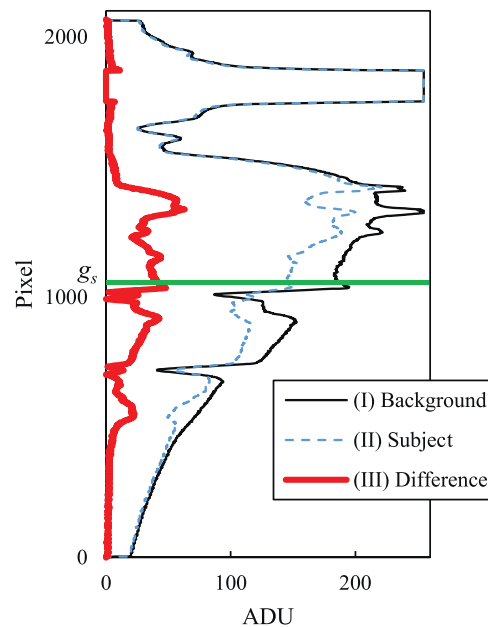
Table 3

Experimental conditions.

Sensor	Horizontal integration detection angle $\theta_i$	26.99 deg
	Vertical movement detection angle $\theta_{MD}$	87.06 deg
	Setting depression angle $\theta_D$	0 deg
	Setting height $H$	90 cm
Subject	Height $h$ (body height)	173 cm
	Width $w$	50 cm
	Color	White
Color of background		White
Illuminance of experimental environment		350 lx



(a) Photo of subject of standing status.



(b) Distribution of Fig. 18(a).

Fig. 18. Experimental situation with subject of standing status and its distribution.

life. These methods should reduce the workload of workers who care for the elderly. The sensor is designed to detect and recognize the status of subjects to reduce the risk of falls within areas where surveillance cameras are not welcome because of privacy issues. The proposed Obrid-Sensor uses a one-dimensional brightness distribution to determine a subject's status and proved reliable in experiments. Thus, this device effectively detection the subject's status without invading their privacy.

To solve the problem of the limited detection range caused by the focal length and size of the rod lens, we propose a slit-type Obrid-Sensor. The detection range can be adjusted by varying the slit design. Comparing with conventional rod-lens-type Obrid-Sensors, the proposed slit-type Obrid-Sensor can be adjusted freely. In addition, the sensor performs as

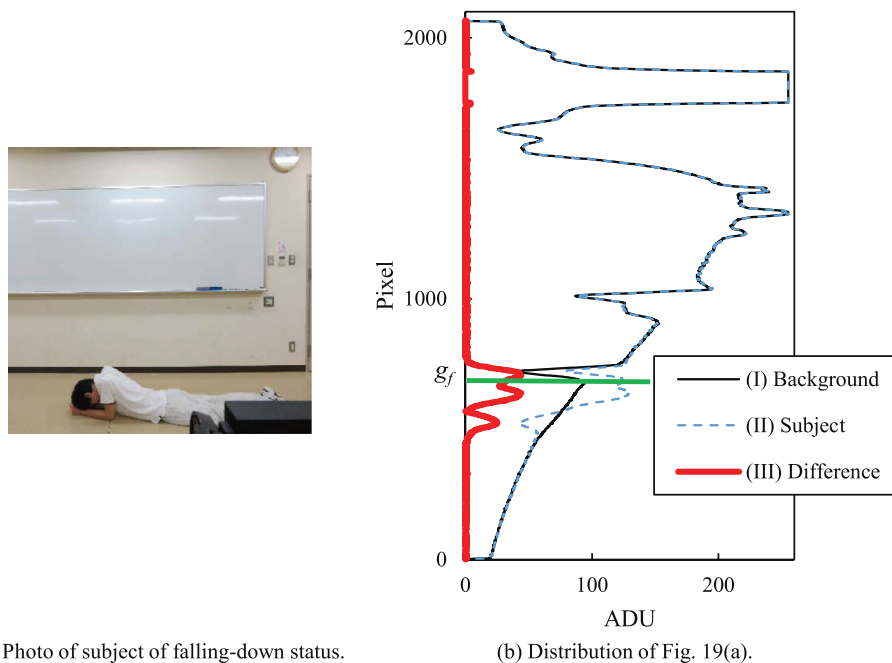


Fig. 19. Experimental situation with subject of falling-down status and its distribution.

well as the rod-lens-type Obrid-Sensor to sense the brightness distribution and to detect the subject. The proposed sensor is simple and can be adjusted depending on the specific application.

In future work, to further advance the medical condition and welfare of elderly, more advanced devices and algorithms will be considered and developed based on this proposed method.

## Acknowledgments

This work was supported by JSPS KAKENHI Grant Number: 15K21197.

## References

- [1] Benezeth Y, Laurent H, Emile B, Rosenberger C. Towards a sensor for detecting human presence and characterizing activity. *Energy Build* 2011;43(2):305–14.
- [2] Paul M, Haque SME, Chakraborty S. Human detection in surveillance videos and its applications—a review. *EURASIP J Adv Signal Process* 2013;43:176.
- [3] Vineet V, Warrell J, Ladicky L, Torr P. Human instance segmentation from video using detector-based conditional random fields. In: *Proceedings of the British Machine Vision Conference*. BMVA Press; 2011. p. 80.1–80.11.
- [4] Lubecke VM, Boric-Lubecke O, Host-Madsen A, Fathy AE. Through-the-wall radar life detection and monitoring. In: *Proceedings of Microwave Symposium*. IEEE; 2007. p. 769–72.
- [5] Rowe MA, Kelly A, Horne C, Lane S, Campbell J, Lehman B, et al. Reducing dangerous nighttime events in persons with dementia by using a nighttime monitoring system. *Alzheimer's Dementia* 2012;5(5):419–26.
- [6] Suzuki S, Matsui T. Remote sensing for medical and health care applications. In: *Remote Sensing-Applications*. InTech; 2012. p. 479–92.
- [7] Kitahara I, Kogure K, Hagita N. Stealth vision: a method for video capturing system with protecting privacy. *IEICE Tech Rep* 2004;103(738):89–94.
- [8] Koshimizu T, Toriyama T, Nishino S, Babaguchi N, Hagita N. Visual abstraction for privacy preserving video surveillance. *IEICE Tech Rep* 2005;105(674):259–302.
- [9] Yabuta K, Kitazawa H, Tanaka T. A fixed monitoring camera image processing method satisfying both privacy protection and object recognition. *IEICE Tech Rep* 2005;105(29):13–18.
- [10] Osada H, Numazawa T, Oka H, Chiba S, Sasaki K, Takahashi M, et al. Construction of pattern displayed telecare system utilizing ferri magnetic infrared sensor. *ITE Tech Rep* 2002;26(14):7–12.
- [11] Mitsutoshi S, Namba Y, Serikawa S. Extraction of values representing human features in order to develop a privacy-preserving sensor. *Int J ICIC* 2008;4(4):883–95.
- [12] Takenouchi T, Morimoto M, Kawahara H, Takahashi M, Yokota H. High-reliability and compact passive infrared detectors monitoring two independent areas. *Matsushita Electr Works Tech Rep* 2004;52(4):62–8.
- [13] Nakashima S, Mu S, Okabe S, Tanaka K, Wakasa Y, Kitazono Y, et al. Restroom human detection using one-dimensional brightness distribution sensor. *Softw Eng, Artif Intell, Network Parallel/Distrib Comput* 2012, *Stud Comput Intell* 2013;492:1–10.

**Shota Nakashima** received the Ph.D. degrees in Electrical Engineering from Kyushu Institute of Technology in 2010, respectively. From 2010 to 2012, he was an Assistant Professor in Ube National College of Technology. Recently, he is a Senior Assistant Professor in Yamaguchi University. His current research interests include image processing, intelligent sensing, and artificial life.

**Shenglin Mu** received the M.E. and Ph.D. degrees in Graduate School of Science and Engineering, Yamaguchi University in 2010 and 2013, respectively. In 2013, he joined National Institution of Technology, Hiroshima College. Now, he is an associate professor in the college. His current research interests include control engineering, esp. intelligent control; soft computing; mechatronics; robotics; and sensing technology.

**Shingo Aramaki** received the B.S. degree from Nishinippon Institute of Technology, Japan, in 2014 and his M.S. degree from Graduate School of Science and Engineering, Yamaguchi University, Japan, in 2016. Currently, he is a Ph.D. student in Graduate School of Sciences and Technology for Innovation, Yamaguchi University. His current research interests include image processing, intelligent sensing, and intelligent control.

**Yuhki Kitazono** received the B.S., M.S., and Ph.D. degrees in Electrical Engineering from Kyushu Institute of Technology in 2007, 2009, and 2011, respectively. From 2011 to 2015, he was an Assistant Professor at National Institute of Technology, Kitakyushu College. Since 2015, he has been an Associate Professor. His current research interests include measurement, sensors, and robotics.

**Kanya Tanaka** graduated from the science and engineering program at the National Defense Academy in 1982. From 1992 through 1998, he was an associate professor of mechanical engineering, Ehime University. He is currently a professor in the Graduate School of Sciences and Technology for Innovation, Yamaguchi University. His main interests are in the theory of intelligent control and related applications.